Spatial Heterogeneity of Low-Grade Gliomas at the Capillary Level: A PET Study on Tumor Blood Flow and Amino Acid Uptake

Matthias T. Wyss[1], Silvia Hofer[2], Martin Hefti[3], Esther Bärtschi[4], Catrina Uhlmann[4], Valerie Treyer[1], and Ulrich Roelcke[5]

[1]PET Center, Division of Nuclear Medicine, University Hospital, Zürich, Switzerland; [2]Department of Oncology, University Hospital, Zürich, Switzerland; [3]Department of Neurosurgery, Cantonal Hospital, Aarau, Switzerland; [4]Department of Oncology and Hematology, Cantonal Hospital, Aarau, Switzerland; and [5]Department of Neurology, Cantonal Hospital, Aarau, Switzerland

Many low-grade gliomas (World Health Organization grade II) respond to chemotherapy. Cerebral blood flow (CBF) and microvessel density may be critical for drug delivery. We used PET with ^{18}F-fluoro-ethyl-L-tyrosine (FET) to measure the spatial distribution of the amino acid carrier, which is located at the brain capillaries, and ^{15}O-H_2O to measure tumor CBF. **Methods:** Seventeen patients with low-grade glioma were studied. Region-of-interest (ROI) analysis was used to quantify tumor tracer uptake, which was normalized to cerebellar uptake (tumor-to-cerebellum ratio). ''Active'' tumor was defined as tumor having a radioactivity concentration that was at least 110% of the cerebellar activity. This threshold provided measures of active tumor volume, global and peak tumor CBF, and ^{18}F-FET uptake. Trace ROIs were applied to create voxelwise profiles of CBF and ^{18}F-FET uptake across tumor and brain. Standard MRI sequences were used for spatial correlations. **Results:** Fourteen of 17 tumors showed increased global CBF and ^{18}F-FET uptake. Active tumor volumes ranged between 3 and 270 cm^3 for ^{18}F-FET and between 1 and 41 cm^3 for CBF. Global ^{18}F-FET uptake in tumors corresponded to CBF increases (Spearman rank $\rho = 0.771$, $P < 0.01$). The volumes of increased CBF and ^{18}F-FET uptake spatially coincided and were also correlated ($\rho = 0.944$, $P < 0.01$). Trace ROIs showed that irrespective of increased ^{18}F-FET uptake at the tumor periphery, CBF increases were more confined to the tumor center. Within individual tumors, spatial heterogeneity was present. Particular tumors infiltrating the corpus callosum showed low CBF and ^{18}F-FET uptake in this tumor region. The patterns observed with PET were not reflected on MRI of the tumors, all of which presented as homogeneous non–gadolinium-enhancing lesions. **Conclusion:** Low-grade gliomas are heterogeneous tumors with regard to the distribution of amino acid uptake and CBF. Both are coupled in the tumor center. At the tumor periphery, where tumor infiltration of surrounding brain occurs, CBF may be low irrespective of increased ^{18}F-FET uptake. An ongoing study is investigating the effect of chemotherapy on these observations.

Key Words: low-grade glioma; fluoro-ethyl-L-tyrosine; blood flow; positron emission tomography

J Nucl Med 2007; 48:1047–1052
DOI: 10.2967/jnumed.106.038489

Most low-grade gliomas affect adults in their third to fifth decades of life. According to the classification of the World Health Organization (WHO), low-grade gliomas (WHO grade II) comprise diffuse astrocytoma, oligodendroglioma, and oligoastrocytoma (*1*). Although the tumors are considered slowly progressing, an annual increase in tumor size of 4.1 mm has been estimated (*2*). Surgery is the standard treatment at the time of first presentation. Subsequent radiotherapy remains controversial (*3,4*). Low-grade gliomas have long been regarded as resistant to chemotherapy; however, several studies published over the last few years showed remarkable responses to regimens such as procarbazine, *N*-(2-chloroethyl)-*N′*-cyclo-hexyl-*N*-nitrosourea, and vincristine or to the alkylating agent temozolomide (*5,6*). There is evidence that loss of heterozygosity on chromosomes 1p and 19q might be predictive of chemotherapy response, but large, prospective randomized studies on this issue are lacking (*6*). On the other hand, the effectiveness of chemotherapy depends on adequate delivery of drugs to tumor cells, and this delivery is a function of drug concentration in the blood, blood flow through tumor microvasculature, and the flux of drugs across tumor capillaries. Our study aimed at the in vivo characterization with PET of microvessel distribution and of cerebral blood flow (CBF) in low-grade gliomas. We used ^{15}O-H_2O as a standard tracer for CBF measurement. To investigate microvessel distribution, we used ^{18}F-fluoro-ethyl-L-tyrosine (FET) as a tracer for amino acid transport (*7*). Several PET studies on human brain tumors showed that the uptake of radiolabeled amino acids is governed by increased influx across the blood–brain barrier (*8–10*). Experimental studies revealed that this influx is mediated by active transendothelial amino acid transport (*11,12*). Accordingly, the signal measured with

Received Nov. 29, 2006; revision accepted Mar. 20, 2007.
For correspondence contact: Ulrich Roelcke, MD, Department of Neurology, Cantonal Hospital, CH 5001 Aarau, Switzerland.
E-mail: roelcke@ksa.ch

^{18}F-FET PET in tumors reflects the magnitude of amino acid transport and its distribution over tumors.

MATERIALS AND METHODS

Patients

We enrolled 17 patients with either progressive or recurrent supratentorial WHO grade II gliomas. At the time of the first surgery (2–127 mo before the PET study), all tumors were histologically verified WHO grade II gliomas and included 5 fibrillary astrocytomas, 7 oligoastrocytomas, and 5 oligodendrogliomas. Recurrence or progression was defined clinically and on MRI and occurred at a mean of 30 mo (range, 2–127 mo; Table 1) after the first tumor surgery. We included only patients who, at the time of our PET study, did not show any gadolinium enhancement on MRI, because this finding may indicate the presence of a more malignant glioma (WHO grade III or IV). The clinical details are presented in Table 1. PET studies were performed within 2 wk of the MRI studies. Written informed consent was obtained from all patients. The study protocol was approved by the local ethics committee.

Image Acquisition and Processing

MRI included standard procedures on a 1.5-T Siemens Magnetom. We obtained digitized pre- and postgadolinium T1- and T2-weighted, proton-density, and fluid-attenuated inversion recovery (FLAIR) sequences (slice thickness, 4.8 mm). Following the methods of recent studies on low-grade gliomas, we used the FLAIR sequences to calculate the tumor volume, because these sequences best delineate between the lesion and adjacent brain (*6,13*).

PET studies were performed on a whole-body PET/CT scanner (Discovery LS; GE Healthcare) and were acquired in 3-dimensional mode with a 14.6-cm axial field of view and a reconstructed in-plane resolution of 7 mm (voxel size, 0.018 cm^3; slice thickness, 4.25 mm). Immediately before the CBF PET study, a low-dose CT scan for attenuation correction was obtained. For the CBF studies, 600–800 MBq of ^{15}O-H_2O were administered using an automatic injection device that delivers the bolus over 20 s. After arrival of the bolus in the brain, acquisition of a series of eighteen 10-s frames was initiated. The ^{15}O-H_2O PET images were transformed according to a previously described approach yielding absolute CBF values without arterial blood sampling (*14*). ^{18}F-FET studies were performed subsequent to the CBF studies within the same session. ^{18}F-FET was produced according to the method of Wester et al. (*15*). For the ^{18}F-FET studies, 140–250 MBq were injected intravenously and tracer accumulation was recorded over 60 min as a series of twelve 5-min frames. To avoid movement of the head during the acquisition, the head was slightly fixed, and PET images were visually assessed for movement artifacts. Attenuation-corrected PET images were reconstructed with standard Fourier rebinning backprojection, including standard calibration factors to receive kBq/mL of tissue and corrections for randoms, scatters, geometry, decay, and dead time. As in other reports (*16*), our patients showed a plateau phase with a relatively stable tissue radioactivity concentration later than 40 min after intravenous tracer injection. Therefore, our ^{18}F-FET PET data were analyzed on averaged activity images acquired 50–60 min after tracer injection. Dividing these activities by the amount of injected activity per kilogram of body weight yielded standardized uptake values.

Data Analysis

PET data were analyzed with PMOD (*17*). As a standard procedure in nuclear medicine, tumor uptake values can be normalized to the contralateral normal brain, allowing easy data analysis

TABLE 1
Patients Ranked by WHO Grade II Histologic Subgroups According to Global ^{18}F-FET T/Cb Ratio

Patient no.	Age (y)	Sex	Histology*	Resection type†	Location	Interval‡ (mo)	Lesion volume (cm^3)			Global T/Cb ratio		Peak T/Cb ratio	
							MRI FLAIR	Active ^{18}F-FET	Active CBF	^{18}F-FET	CBF	^{18}F-FET	CBF
1	39	M	FIAC	b	Temporal, R	19	34	—	—	0.77	0.77	—	—
2	49	F	FIAC	p	Frontoparietal, L	127	46	29	12	1.24	1.25	1.39	1.45
3	46	F	FIAC	p	Temporooccipital, R	9	40	6	1	1.24	1.21	1.40	—
4	51	F	FIAC	p	Frontotemporal, L	79	88	65	9	1.24	1.39	1.38	1.69
5	34	M	FIAC	p	Temporal, L	27	44	6	1	1.25	1.19	1.39	—
6	55	M	OA	b	Temporal, R	12	56	—	—	0.70	0.59	—	—
7	56	M	OA	gt	Frontal, R	81	91	3	1	1.21	1.31	1.24	—
8	31	F	OA	p	Frontal, L	40	14	11	5	1.32	1.34	1.58	1.61
9	27	M	OA	p	Temporal, L	6	23	18	1	1.42	1.25	1.78	—
10	39	M	OA	b	Temporal, L	9	79	64	16	1.44	1.33	1.93	1.59
11	42	M	OA	p	Frontotemporal, R	50	44	23	10	1.50	1.51	2.18	1.96
12	28	M	OA	b	Parietal, L	5	90	79	28	1.59	1.49	2.17	1.93
13	50	F	OD	p	Frontal, L	26	23	—	—	0.61	0.45	—	—
14	54	F	OD	b	Temporal, L	2	42	6	1	1.28	1.23	1.46	—
15	37	M	OD	b	Frontal, L, R	13	140	270	41	1.33	1.25	1.62	1.41
16	45	F	OD	b	Frontal, L	2	25	27	3	1.40	1.20	1.75	—
17	34	M	OD	b	Temporal, L	6	23	28	9	1.65	1.35	2.25	1.76

*FIAC = fibrillary astrocytoma; OA = oligoastrocytoma; OD = oligodendroglioma.
†b = biopsy; p = partial; gt = gross total resection.
‡Between surgery and PET.
— = no active tumor volume (in those patients, ROIs for calculation of global uptake ratio were drawn from MRI FLAIR images).

and reliable interindividual comparisons. However, normalization to contralateral brain depends on the location of the tumor in the brain and may thus infer substantial variation, particularly as 2 tumors in our series crossed the midline. We therefore chose the cerebellum as the reference region because it is a large and homogeneous structure and was distant from the tumor. Regions of interest (ROIs) were first placed over both sides of the cerebellum on 3 subsequent slides. The mean activity of all cerebellar ROIs was used to set the threshold for normalization of tumor tracer uptake (tumor-to-cerebellum [T/Cb] ratio). This thresholding procedure has recently been proposed to provide an observer-independent evaluation, which is particularly important for follow-up PET studies during tumor treatment (*18*). In a first step, we used thresholds between 100% and 120% of cerebellar activity. Increasing the threshold produced moderate decreases of active tumor volumes and small increases of T/Cb ratios. We finally chose a threshold that gave a volume of active voxels close to what was the "visibly increased" ^{18}F-FET uptake. For our low-grade gliomas, we found this threshold to be 110%. This threshold was also applied for the quantification of CBF. Accordingly, tumor ROIs were placed covering all voxels with activity values above 110% of the mean activity in the cerebellum, thus yielding the active tumor volume for CBF and ^{18}F-FET uptake. The activity in these tumor ROIs was then used for the calculation of global T/Cb ratios (all active voxels) and peak T/Cb ratios (all voxels that were 75% or more of the maximum radioactivity in the tumor ROI). In tumors with inactive tumor volumes (below 110% of the mean activity in the cerebellum), digitized MRI FLAIR images were coregistered with the PET studies to define the placement of tumor ROIs according to the FLAIR lesion volume.

To more precisely investigate the spatial relationship between ^{18}F-FET uptake and CBF, we placed linear trace ROIs that spanned from normal cortex through white matter and tumor and created CBF and ^{18}F-FET profiles across the brain (Fig. 1, yellow line). First, trace ROIs were placed on the 3 adjacent planes that showed the highest tumor tracer uptake. For each of these planes, 3 adjacent parallel trace ROIs were created per plane in the ^{18}F-FET study and were then also used at the same position for the coregistered CBF studies. Depending on the individual tumor location, a single trace ROI consisted of up to 64 voxels (voxel size, 0.018 cm^3). At this step, 9 single ^{18}F-FET and CBF profiles per patient were available. Second, the activity of the spatially corresponding voxels derived from these 9 profiles was averaged and yielded a mean trace ROI profile for ^{18}F-FET and CBF activity for each patient. Then, the mean activity for each voxel was normalized to the cerebellum. Accordingly, the data points of these profiles represent voxel averages of T/Cb ratios for CBF and ^{18}F-FET uptake (*y*-axis) and the distance (mm) across the brain (*x*-axis).

Statistics

The Spearman rank test was used to search for correlations between the active tumor volumes of CBF and ^{18}F-FET uptake, between tumor uptake of ^{18}F-FET and tumor CBF, and between these measures and the MRI FLAIR lesion.

RESULTS

The results are summarized in Table 1. Relative to normal brain, we found increased ^{18}F-FET uptake and CBF in 14 of 17 tumors. ^{18}F-FET uptake and CBF were not homogeneously increased across these tumors but rather showed a variable distribution. The peaks of CBF and ^{18}F-FET uptake were spatially colocalized. In 3 tumors, both ^{18}F-FET uptake and CBF were decreased relative to normal brain. The heterogeneity of ^{18}F-FET uptake and CBF within individual

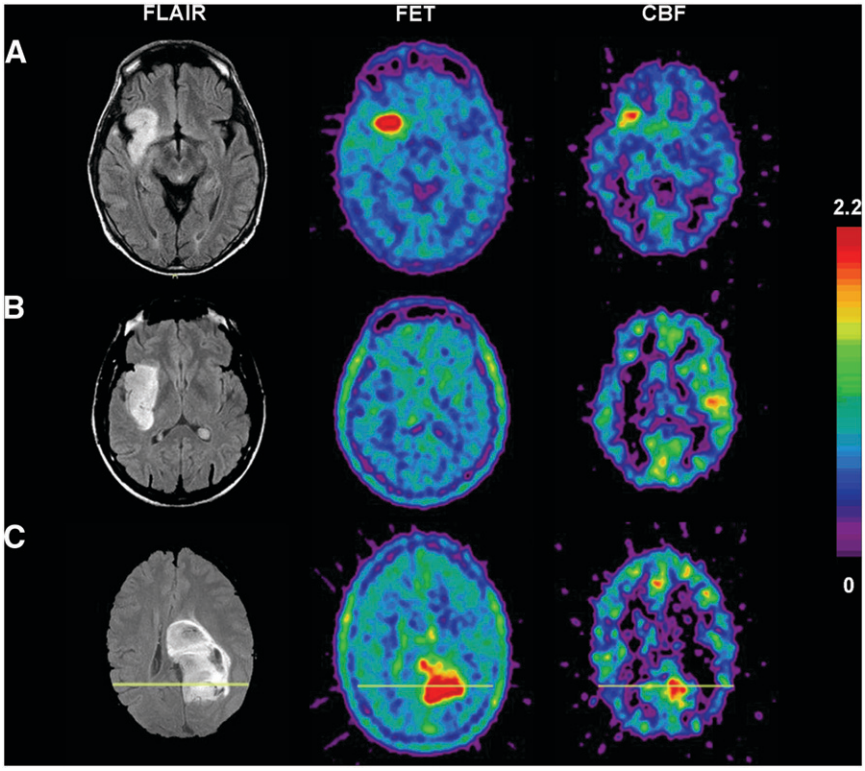

FIGURE 1. Heterogeneity of ^{18}F-FET uptake and CBF in 3 low-grade gliomas. Corresponding axial slices are presented. Color scale represents T/Cb ratio of ^{18}F-FET and CBF. (A) Oligoastrocytoma shows markedly increased ^{18}F-FET uptake and CBF in right frontoinsular region (patient 11 in Table 1). ^{18}F-FET and CBF peak uptake regions coincide; however, active volume of CBF is smaller than active ^{18}F-FET volume. (B) Reduced ^{18}F-FET uptake and CBF in fibrillary astrocytoma (patient 1). (C) Oligoastrocytoma (patient 12). Anterior tumor part involves corpus callosum and shows substantially reduced CBF and ^{18}F-FET uptake when compared with posterior tumor part. This heterogeneity is not evident from any MRI sequences. Yellow line through posterior part of brain and tumor illustrates positioning of trace ROI (Fig. 4).

tumors and within our group of low-grade gliomas is illustrated in Figure 1.

Tumor tracer uptake was quantified by normalizing the tumor radioactivity concentration to the activity of the cerebellum (uptake ratio). Cerebellar ^{18}F-FET uptake and CBF were calculated as the mean value of both cerebellar hemispheres. Asymmetry between the hemispheres ("crossed cerebellar diaschisis") was less than 5% for ^{18}F-FET and less than 9% for CBF. For the cerebellum, the ^{18}F-FET standardized uptake value was 1.22 ± 0.32 (mean ± SD). The cerebellar CBF was 36.4 ± 8.6 mL/min/100 mL. At a 110% cutoff of cerebellar tracer uptake, tumor uptake ratios varied between 0.61 and 1.65 for global ^{18}F-FET uptake and between 1.24 and 2.25 for peak ^{18}F-FET uptake. For CBF, these values ranged from 0.45 to 1.50 for the global ratio and from 1.41 to 1.96 for the peak ratio. At lower ^{18}F-FET uptake ratios (global), smaller variations in CBF ratios were observed, whereas for higher ^{18}F-FET uptake ratios (peak), the variation in CBF ratios increased (Fig. 2). Uptake ratios tended to be higher in oligodendroglial tumors than in fibrillary astrocytoma. No correlation between MRI lesion volume and tracer uptake was observed (^{18}F-FET: Spearman rank $\rho = 0.023$, $P = 0.931$; CBF: Spearman rank $\rho = 0.262$, $P = 0.309$) (Table 1). Over the whole study population, ^{18}F-FET uptake and CBF correlated (Fig. 2): For global uptake ratios, the Spearman rank correlations were $\rho = 0.771$, $P < 0.01$ ($n = 17$). Because of the small number of pairs, the correlation of peak uptake ratios did not reach statistical significance ($\rho = 0.571$, $P = 0.139$).

In most tumors, the volume of increased ^{18}F-FET uptake was smaller than the corresponding tumor volume on MRI FLAIR images. Active tumor volumes of ^{18}F-FET and CBF were colocalized within 1 tumor (Fig. 1); however, the CBF volume was always smaller than the ^{18}F-FET uptake volume. The active tumor volumes ranged from 3 to 270 cm^3 for ^{18}F-FET and from 1 to 41 cm^3 for CBF. The correlation between active global tumor volumes is presented in Figure 3 (Spearman rank $\rho = 0.944$, $P < 0.01$). To address this spatial relationship between intratumoral tracer uptake, we created CBF and ^{18}F-FET profiles across tumor and brain. The positioning of trace ROIs is illustrated for a single patient (patient 12) in Figure 1. The resulting profile of ^{18}F-FET and CBF distribution is exemplified in Figure 4. The presented pattern was observed in all 14 tumors with increased ^{18}F-FET uptake and CBF—that is, the peak coincidence of ^{18}F-FET uptake and CBF. Reflective of our active volume data, the area under the curve in the trace ROIs was smaller for the tumor CBF than for the tumor ^{18}F-FET uptake profiles. Along the profiles, the mean distance between increase of intratumoral ^{18}F-FET uptake and CBF was 6.3 mm (range, 2.2–13.6 mm). At the position where the CBF ratio in tumors started to exceed 1.0, the mean ^{18}F-FET ratio was 1.51 (1.01–2.24).

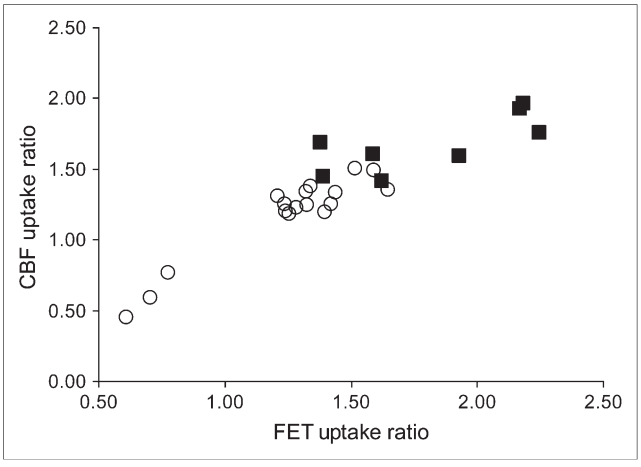

FIGURE 2. Distribution of global (○) and peak (■) ^{18}F-FET uptake and CBF. Values represent T/Cb ratios.

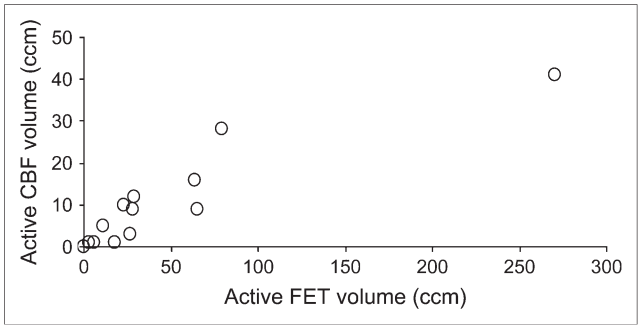

FIGURE 3. Correlation of global active tumor volumes of ^{18}F-FET and CBF (Spearman rank $\rho = 0.944$, $P < 0.01$). Significant correlation is maintained if outlier is excluded from analysis ($\rho = 0.885$, $P < 0.01$).

DISCUSSION

Our study demonstrated a substantial heterogeneity in CBF and ^{18}F-FET uptake over the whole series of low-grade gliomas that, on MRI, appeared as homogeneous

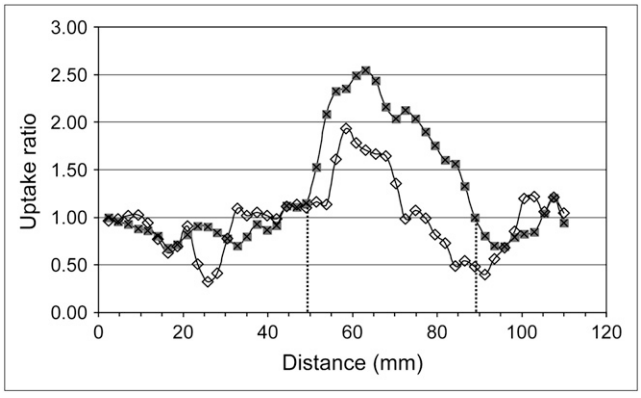

FIGURE 4. Trace ROI analysis in a single patient (patient 12). Pixelwise profiles of ^{18}F-FET uptake (■) and CBF (◇) span from normal cortex over white matter and tumor. Vertical dashed lines represent tumor borders on MRI (patient 12; Fig. 1C). Increases of tumor CBF (T/Cb ratio > 1.0) are more confined to tumor center. T/Cb ratio increases in this patient at a ratio of approximately 2.1 of ^{18}F-FET uptake.

non–gadolinium-enhancing lesions. In many patients, we also observed intratumoral heterogeneity on the PET studies, possibly indicating that subregions of tumors could behave differentially with respect to tumor evolution and treatment response. Knowledge of the individual tumor vasculature is of particular interest with regard to angiogenetic tumor potential and targeted treatment. The total intravascular volume, which comprises all sizes of tumor vessels, can be used as an in vivo marker of angiogenesis and can be studied by following the changes in the MRI signal after administration of gadolinium (*19,20*). If the point of interest is the distribution of the capillaries themselves, where solutes and drugs are exchanged, markers should exclusively trace mechanisms located at that anatomic level. Such is the case for radiolabeled amino acids that bind to and are transported by the amino acid carriers located in the endothelial cells of the blood–brain barrier (*21*). In brain tumors of various WHO grades, uptake of ^{11}C-methyl-L-methionine correlates with the microvascular density (MVD) as validated by immunohistochemistry (*22*). ^{18}F-FET is a nonmetabolized tyrosine analog and behaves similarly to methionine (*16*). ^{18}F-FET was evaluated for the clinical investigation of gliomas (*7,16*). We found an ^{18}F-FET uptake ratio of between 0.61 and 1.65 for the whole tumor and peak values of between 1.24 and 2.25. These ratios are in the range of the data presented by Kracht et al. (*22*). Taking these findings together, our results provide evidence that ^{18}F-FET, like methionine, is a surrogate marker of MVD. To validate this assumption, we initiated a study on ^{18}F-FET PET–guided biopsies and determination of MVD in patients with low-grade gliomas.

In our series, 3 of 17 tumors showed neither increased tyrosine uptake nor increased CBF. In addition, tumor areas contacting or infiltrating the corpus callosum exhibited normal or reduced CBF and ^{18}F-FET uptake, whereas in the same tumor, distant cortical or subcortical areas showed increases of these measures (Fig. 1). Our finding of reduced ^{18}F-FET uptake in some tumors would be in line with immunohistochemical results on microvessel counts in astrocytomas. In particular, low-grade astrocytomas may show MVDs below the level of normal cortex or white matter (*23*). Studies have shown that microvessels in these tumors are native cerebral vessels co-opted by tumor cells and that the formation of new vessels ("neo-angiogenesis") and higher vessel densities occur in more malignant tumors (*23,24*).

Earlier studies on CBF in gliomas reported a similar range for tumors (7–102 mL/100 mL/min) and for normal white matter and cortex (15–59 mL/100 mL/min) (*25–27*). The magnitude of CBF in these studies did not discriminate between glioma types or WHO grade. Across our series, tumor CBF and ^{18}F-FET uptake correlated (Fig. 2). Our data therefore suggest a coupling between blood flow and microvascular distribution in low-grade gliomas. This coupling is different from known perfusion patterns in more malignant gliomas (WHO grades III and IV), in which, irrespective of the high vascularity, low CBF is considered to be responsible for the formation of hypoxia (*28*). In addition, we found a significant correlation between active ^{18}F-FET and perfused tumor volumes (Fig. 3). ^{18}F-FET and CBF volumes showed a close spatial coincidence and were independent of lesion size on MRI (Fig. 1). Interestingly, the active CBF volumes were smaller than the corresponding ^{18}F-FET volumes (Table 1), as is explained by the characteristic intratumoral rises in ^{18}F-FET uptake and CBF as presented in the trace ROI analysis (Fig. 4). Our data revealed that CBF increases occurred when uptake of ^{18}F-FET exceeded a certain level (mean ratio, 1.50). Assuming that ^{18}F-FET uptake is related to MVD, our results can be transferred into absolute numbers of tumor MVD by comparison with the data presented by Kracht et al. (*22*). They reported global ^{11}C-methyl-L-methionine uptake ratios of 1.30 ± 0.20 for astrocytic tumors and 2.30 ± 0.35 for oligodendroglial tumors (WHO grade II)—values that are similar to our ^{18}F-FET uptake values (Table 1). Correlating ^{11}C-methyl-L-methionine uptake and histopathologically proven MVD, an amino acid uptake ratio of 1.50 equals 10 microvessels/0.763 mm^2 (*22*). If we extrapolate a median ^{18}F-FET uptake ratio of 1.50 as calculated from our trace ROIs, an approximate MVD of 13 microvessels/mm^2 would result. At this level, CBF starts to increase above the level in normal brain. In view of that fact, we assume that CBF increases follow the formation of new microvessels and therefore represent a subsequent phenomenon.

Intratumoral heterogeneity of tumor CBF and amino acid uptake has been reported in several animal studies. In opposition to our findings, CBF progressively increased from the tumor center to the tumor periphery and to brain surrounding the tumor (*29*). A corresponding increase in MVD was reported for large tumors of the same tumor model (tumor center, 245/mm^2, vs. surrounding brain, 689/mm^2) (*30*). With regard to a cortical or subcortical tumor location, variable amino acid uptake values were found in more "malignant" tumor models (*11*). In humans, intratumoral variations have not been recognized so far. Overall, we detected in our study no differences in ^{18}F-FET uptake or CBF with regard to cortical or subcortical tumor location. However, we noted intratumoral heterogeneity, particularly in tumor regions infiltrating the corpus callosum. Low CBF and capillary density may initiate the development of a mismatch between metabolic demand and energy supply and may promote hypoxia, possibly making these tumors prone to behaving more aggressively than tumors with the same histopathologic features located outside the corpus callosum (*31*).

CONCLUSION

Taking our observations together, we found that tumor CBF and amino acid uptake varied substantially in nonenhancing WHO grade II gliomas. This variation was evident within the whole group of tumors and within individual tumors and did not depend on lesion size on MRI. All patients were studied at the time of clinical or radiologic progression, making tumor therapy necessary after initial

surgery and observation. Because MVD constitutes a significant independent prognostic factor (*32,33*), it is tempting to validate whether ^{18}F-FET PET provides a robust means for the in vivo measurement of MVD. Our results in this study led us to initiate a prospective PET study that will address the effect of chemotherapy on regional tumor blood flow and amino acid uptake, with particular emphasis on the tumor-to-brain border zone, because this is the area most critical to tumor cell infiltration of the surrounding brain and to tumor progression and the prognosis of patients with low-grade gliomas.

ACKNOWLEDGMENTS

This study was supported by grants from the Swiss Group for Clinical Cancer Research (SAKK) and by Essex Chemie AG, Luzern, Switzerland. We thank Tibor Cservenyak for radiotracer production.

REFERENCES

1. Kleihues P, Cavanee WK. *Pathology and Genetics of Tumours of the Nervous System*. Lyon, France: IARC Press; 2000:10–21.
2. Mandonnet E, Delattre JY, Tanguy ML, et al. Continuous growth of mean tumor diameter in a subset of grade II gliomas. *Ann Neurol.* 2003;53:524–528.
3. Van den Bent MJ, Afra D, de Witte O, et al. Long-term efficacy of early versus delayed radiotherapy for low-grade astrocytoma and oligodendroglioma in adults: the EORTC 22845 randomised trial. *Lancet.* 2005;366:985–990.
4. Van den Bent MJ. Advances in the biology and treatment of oligodendrogliomas. *Curr Opin Neurol.* 2004;17:675–680.
5. Brada M, Viviers L, Abson C, et al. Phase II study of primary temozolomide chemotherapy in patients with WHO grade II gliomas. *Ann Oncol.* 2003;14:1715–1721.
6. Hoang-Xuan K, Capelle L, Kujas M, et al. Temozolomide as initial treatment for adults with low-grade oligodendrogliomas or oligoastrocytomas and correlation with chromosome 1p deletions. *J Clin Oncol.* 2004;22:3133–3138.
7. Weckesser M, Langen KJ, Rickert CH, et al. O-(2-[^{18}F]fluorethyl)-L-tyrosine PET in the clinical evaluation of primary brain tumours. *Eur J Nucl Med Mol Imaging.* 2005;32:422–429.
8. Wienhard K, Herholz K, Coenen HH, et al. Increased amino acid transport into brain tumors measured by PET of L-(2-^{18}F)fluorotyrosine. *J Nucl Med.* 1991;32:1338–1346.
9. Roelcke U, Radu E, Ametamey S, Pellikka R, Steinbrich W, Leenders KL. Association of rubidium and C-methionine uptake in brain tumors measured by positron emission tomography. *J Neurooncol.* 1996;27:163–171.
10. Heiss P, Mayer S, Herz M, Wester HJ, Schwaiger M, Senekowitsch-Schmidtke R. Investigation of transport mechanism and uptake kinetics of O-(2-[^{18}F]fluoroethyl)-L-tyrosine in vitro and in vivo. *J Nucl Med.* 1999;40:1367–1373.
11. Miyagawa T, Oku T, Uehara H, et al. "Facilitated" amino acid transport is upregulated in brain tumors. *J Cereb Blood Flow Metab.* 1998;18:500–509.
12. Langen KJ, Jarosch M, Mühlensiepen H, et al. Comparison of fluorotyrosines and methionine uptake in F98 rat gliomas. *Nucl Med Biol.* 2003;30:501–508.
13. Husstedt HW, Sickert M, Kostler H, Haubitz B, Becker H. Diagnostic value of the fast-FLAIR sequence in MR imaging of intracranial tumors. *Eur Radiol.* 2000;10:745–752.
14. Treyer V, Jobin M, Burger C, Teneggi V, Buck A. Quantitative cerebral $H_2{}^{15}O$ perfusion PET without arterial blood sampling, a method based on washout rate. *Eur J Nucl Med Mol Imaging.* 2003;30:572–580.
15. Wester HJ, Herz M, Weber W, et al. Synthesis and radiopharmacology of O-(2-[^{18}F]fluoroethyl)-L-tyrosine for tumor imaging. *J Nucl Med.* 1999;40:205–212.
16. Weber WA, Wester HJ, Grosu AL, et al. O-(2-[^{18}F]fluoroethyl)-L-tyrosine and L-[methyl-^{11}C]methionine uptake in brain tumours: initial results of a comparative study. *Eur J Nucl Med.* 2000;27:542–549.
17. Mikolajczyk K, Szabatin M, Rudnicki P, Grodzki M, Burger CA. JAVA environment for medical image data analysis: initial application for brain PET quantitation. *Med Inform (Lond).* 1998;23:207–214.
18. Tang BN, Sadeghi N, Branle F, De Witte O, Wikler D, Goldman S. Semiquantification of methionine uptake and flair signal for the evaluation of chemotherapy in low-grade oligodendroglioma. *J Neurooncol.* 2005;71:161–168.
19. Rosen BR, Belliveau JW, Vevea JM, Brady TJ. Perfusion imaging with NMR contrast agents. *Magn Reson Med.* 1990;14:249–265.
20. Abu-Hajir M, Rand SD, Krouwer HG, Schmainda KM. Noninvasive assessment of neoplastic angiogenesis: the role of magnetic resonance imaging. *Semin Thromb Hemost.* 2003;29:309–315.
21. Christensen HN. Role of amino acid transport and countertransport in nutrition and metabolism. *Physiol Rev.* 1990;70:43–77.
22. Kracht LW, Friese M, Herholz K, et al. Methyl-[^{11}C]-L-methionine uptake as measured by positron emission tomography correlates to microvessel density in patients with glioma. *Eur J Nucl Med Mol Imaging.* 2003;30:868–873.
23. Wesseling P, van der Laak JA, Link M, Teepen HL, Ruiter DJ. Quantitative analysis of microvascular changes in diffuse astrocytic neoplasms with increasing grade of malignancy. *Hum Pathol.* 1998;29:352–358.
24. Fischer I, Gagner JP, Law M, Newcomb EW, Zagzag D. Angiogenesis in gliomas: biology and molecular pathophysiology. *Brain Pathol.* 2005;15:297–310.
25. Lammertsma AA, Wise RJ, Cox TC, Thomas DG, Jones T. Measurement of blood flow, oxygen utilisation, oxygen extraction ratio, and fractional blood volume in human brain tumours and surrounding oedematous tissue. *Br J Radiol.* 1985;58:725–734.
26. Mineura K, Sasajima T, Kowada M, et al. Perfusion and metabolism in predicting the survival of patients with cerebral gliomas. *Cancer.* 1994;73:2386–2394.
27. Mineura K, Shioya H, Kowada M, Ogawa T, Hatazawa J, Uemura K. Blood flow and metabolism of oligodendrogliomas: a positron emission tomography study with kinetic analysis of ^{18}F-fluorodeoxyglucose. *J Neurooncol.* 1999;43:49–57.
28. Bruehlmeier M, Roelcke U, Schubiger PA, Ametamey SM. Assessment of hypoxia and perfusion in human brain tumors using PET with ^{18}F-fluoromisonidazole and ^{15}O-H_2O. *J Nucl Med.* 2004;45:1851–1859.
29. Blasberg RG, Kobayashi T, Horowitz M, et al. Regional blood-to-tissue transport in ethylnitrosourea-induced brain tumors. *Ann Neurol.* 1983;14:202–215.
30. Schlageter KE, Molnar P, Lapin GD, Groothuis DR. Microvessel organization and structure in experimental brain tumors: microvessel populations with distinctive structural and functional properties. *Microvasc Res.* 1999;58:312–328.
31. Pignatti F, van den Bent M, Curran D, et al. Prognostic factors for survival in adult patients with cerebral low-grade glioma. *J Clin Oncol.* 2002;20:2076–2084.
32. Leon SP, Folkerth RD, Black PM. Microvessel density is a prognostic indicator for patients with astroglial brain tumors. *Cancer.* 1996;77:362–372.
33. Abdulrauf SI, Edvardsen K, Ho KL, Yang XY, Rock JP, Rosenblum ML. Vascular endothelial growth factor expression and vascular density as prognostic markers of survival in patients with low-grade astrocytoma. *J Neurosurg.* 1998;88:513–520.

The Journal of NUCLEAR MEDICINE

Spatial Heterogeneity of Low-Grade Gliomas at the Capillary Level: A PET Study on Tumor Blood Flow and Amino Acid Uptake

Matthias T. Wyss, Silvia Hofer, Martin Hefti, Esther Bärtschi, Catrina Uhlmann, Valerie Treyer and Ulrich Roelcke

J Nucl Med. 2007;48:1047-1052.
Published online: June 15, 2007.
Doi: 10.2967/jnumed.106.038489

The Journal of Nuclear Medicine is published monthly.
SNMMI | Society of Nuclear Medicine and Molecular Imaging
1850 Samuel Morse Drive, Reston, VA 20190.
(Print ISSN: 0161-5505, Online ISSN: 2159-662X)

SNMMI SOCIETY OF NUCLEAR MEDICINE AND MOLECULAR IMAGING